Systems/Circuits

Dynorphinergic Projections from the Central Amygdala to the Parabrachial Nucleus Regulate Itch

Hideki Funahashi,[1,2*] Darya Pavlenko,[1*] Kent Sakai,[1] Rebecca Verpile,[1] Kristen M. Sanders,[1] and Tasuku Akiyama[1]
[1]Dr. Phillip Frost Department of Dermatology and Cutaneous Surgery and Miami Itch Center, University of Miami Miller School of Medicine, Miami, FL 33136 and [2]Department of Psychiatry, Faculty of Medicine, University of Miyazaki, Miyazaki City, Miyazaki 5200, Japan

The amygdala plays a key role in the processing of itch and pain signals as well as emotion. A previous study revealed that the central nucleus of the amygdala (CeA)-parabrachial nucleus (PBN) pathway is involved in pain regulation. The same pathway might also control itch. To test this possibility, prodynorphin (Pdyn)-Cre mice were used to optogenetically manipulate Pdyn$^+$ CeA-to-PBN projections. We found that optogenetic stimulation of Pdyn$^+$ amygdala neurons or Pdyn$^+$ CeA-to-PBN projections inhibited histamine-evoked and chloroquine-evoked scratching. The number of Fos-positive neurons in the PBN increased following intradermal injection of chloroquine. Optogenetic stimulation of Pdyn$^+$ CeA-to-PBN projections suppressed the increase in Fos expression in the PBN. Optogenetic stimulation of Pdyn$^+$ CeA-to-PBN projections increased thermal and mechanical thresholds without affecting anxiety-like behavior. These results highlight the importance of dynorphinergic projections from the central amygdala to the parabrachial nucleus in the regulation of itch signaling.

Key words: **amygdala; anxiety; itch; mice; pain; parabrachial nucleus**

Significance Statement

The central nucleus of the amygdala (CeA)-parabrachial nucleus (PBN) pathway regulates pain signaling. Using prodynorphin (Pdyn)-cre mice, we investigated the role of Pdyn$^+$ CeA-to-PBN projections in itch. Optogenetic stimulation of Pdyn$^+$ CeA-to-PBN projections inhibited pruritogen-evoked scratching and neuronal activity (c-Fos expression) in the PBN. Together, dynorphinergic projections from the central amygdala to the parabrachial nucleus are important for regulating itch information.

Introduction

The amygdala, the major center for the generation of anxiety and fear, plays key roles in mediating the affective component of itch and pain (Neugebauer, 2015; Sanders and Akiyama, 2018; Sanders et al., 2019; Samineni et al., 2021). Brain imaging studies have shown that the amygdala is activated by both histamine-dependent and histamine-independent itch stimuli as well as painful stimuli (Papoiu et al., 2012; Simons et al., 2014; Vierow et al., 2015; Mochizuki et al., 2020). The amygdala integrates direct and indirect nociceptive input from many brain regions, including the parabrachial nucleus (PBN) and the thalamus, to trigger behavioral responses (Han et al., 2015; Cai et al., 2018; Campos et al., 2018; Chiang et al., 2020; Deng et al., 2020; Li and Sheets, 2020). However, the precise mechanism by which amygdala neurons integrate pruriceptive and nociceptive inputs is unknown.

Recent research has identified two distinct populations of the central nucleus of the amygdala (CeA) neurons with antinociceptive functions. One population expresses somatostatin and prodynorphin (Pdyn; Kim et al., 2017; Wilson et al., 2019), whereas the other is activated by general anesthetics and contributes to their analgesic effects (Hua et al., 2020). While the CeA projects to many brain regions, a recent study found that CeA-to-PBN-projecting neurons regulate pain signaling (Raver et al., 2020; Hogri et al., 2022). The CeA-to-PBN-projecting neurons contain dynorphin, somatostatin, corticotropin-releasing hormone, nociceptin, neurotensin, and 5-hydroxytryptamine receptor 2A (Hardaway et al., 2019; Bartonjo and Lundy, 2020; Raver et al., 2020; Torruella-Suárez et al., 2020). Fluorescence in situ hybridization experiments revealed that a large proportion of the CeA-to-PBN-projecting neurons expressed dynorphin (Raver et al., 2020). Furthermore, it has been reported that injection of a $GABA_A$ agonist into the CeA suppressed acute and chronic itch (Chen et al., 2016). To date, however, little research has been

Received Apr. 23, 2023; revised June 19, 2023; accepted June 22, 2023.

Author contributions: T.A. designed research; H.F., D.P., K.S., R.V., K.M.S., and T.A. performed research; H.F., D.P., and T.A. analyzed data; H.F., D.P., and T.A. edited the paper; T.A. wrote the first draft of the paper; T.A. wrote the paper.

This project was supported by grants from the National Institutes of Health Grant R01AR074062 and the Stanley Glaser Foundation Research Award UM SJG 2019-18 (to T.A.). We thank Kevin Johnson (University of Miami) for his generous technical support and Gabriella Guerriero (University of Miami) for her contribution.

*H.F. and D.P. contributed equally to this work.

The authors declare no competing financial interests.

Correspondence should be addressed to Tasuku Akiyama at takiyama@miami.edu.

https://doi.org/10.1523/JNEUROSCI.0726-23.2023

conducted into the role of the CeA-to-PBN projections in the regulation of itch.

Here, we selectively stimulated the Pdyn$^+$ CeA-to-PBN projections using the Pdyn-Cre mouse line to express the light-sensitive cation channel chrimsonR in the Pdyn$^+$ CeA-to-PBN projections. We investigated the roles of Pdyn$^+$ CeA-to-PBN projections in the regulation of itch.

Materials and Methods

Mice

All procedures were approved by the Institutional Animal Care and Use Committees of the University of Miami. Pdyn-Cre mice (B6;129S-Pdyn$^{tm1.1(cre)Mjkr}$ 027958) and C57BL/6J mice were obtained from The Jackson Laboratory.

All mice were group housed (two to five per cage), given standard food and water *ad libitum*, and maintained under a 12/12 h light/dark cycle (6 A.M. lights on, 6 P.M. lights off). All mice were habituated to handling by the experimenter, intradermal PBS and pruritogen injection, and to the testing room. A small area of fur on the rostral back was shaved for intradermal injections. Adult male and female mice were randomly assigned to experimental groups. No sex differences were noted for any quantified data. Therefore, sexes of the same genotype were pooled for analysis. All mice were at least eight weeks old at the time of experiments. Mice were randomly assigned to experimental groups. Mice were typically used for a battery of behavioral tests, with a one-week break between each test. In every experiment, care was taken to minimize external sources of stress to the mice.

Adeno-associated virus injection

Mice were anesthetized with isoflurane (3%) and positioned in a stereotaxic frame. An adeno-associated virus (AAV) encoding a Cre-dependent fast opsin (ChrimsonR; Klapoetke et al., 2014) fused to enhanced red fluorescent protein (pAAV5/Syn-FLEX-ChrimsonR-tdTomato; Addgene; created by Ed Boyden, MIT; Addgene viral prep #62723-AAV5; RRID: Addgene_62723) was bilaterally injected into the CeA [coordinates: anterior-posterior (AP) −1.34 mm, medial-lateral (ML) ±2.7 mm, dorsal-ventral (DV) −4.5 mm]. Control mice received bilateral injections of AAV5/phSyn1(S)-FLEX-tdTomato [a gift from Hongkui Zeng (Addgene plasmid #51505; RRID:Addgene_51505); Oh et al., 2014]. Control groups were studied independently from other experimental groups. The injection volume was 0.25 μl, injected over 1 min using a glass needle and plunger. The viral dose was 8.5×10^{12} vector genomes/ml. For amygdala stimulation, an optic fiber (200 μm in diameter, 3.5 mm) was implanted directly above each injection site and fixed to the skull with dental cement. For PBN stimulation, optic fibers (200 μm in diameter, 3 mm) were implanted following stereotaxic coordinates: AP −5 mm; ML ±1.4 mm. Mice were allowed three weeks to recover from surgery before behavior testing.

Optogenetic stimulation

For optic stimulation, double flexible fiber patch cords were attached to the external ends of the optic fibers and connected to an LED light source (Thorlabs) that delivered yellow light (554-nm wavelength) capable of activating ChrimsonR. Light pulses were delivered at constant intensity and frequency (2.0 mW, 2 Hz) via an LED driver connected to a waveform generator. Light intensity was measured in each fiber using an optical power meter (Thorlabs). For behavior testing, mice were briefly anesthetized with isoflurane (3%) to connect implanted optic fibers to the patch cords. Mice were habituated to cable attachment for 1 h before testing.

Scratching behavior

All behavioral testing was conducted between 9 A.M and 6 P.M. Each apparatus was constructed of acrylic plastic (Interstate Plastics) and cleaned with 70% ethanol between mice to minimize odor effects. Each mouse was habituated to the recording chamber (15 × 15 cm) before testing.

Histamine (50 μg/10 μl; Sigma-Aldrich) or chloroquine diphosphate salt (100 μg/10 μl; Sigma-Aldrich) was injected intradermally into the shaved rostral back skin with ("ON") and without ("OFF") continuous bilateral yellow light stimulation (2.0 mW, 2 Hz). The light was turned on until the end of the behavior test. The time interval between experiments with ON and OFF conditions was four weeks. We observed that the weight and/or stress of the cable attachment for optogenetic stimulation suppressed the scratch response. Importantly, the cable was still attached in the OFF condition to allow us to control for this effect. Injections were made using a 30G needle connected to a microsyringe (Hamilton Company) via PE-50 tubing (Instech Laboratories). Behavior was video recorded for 30 min. The number of scratch bouts was analyzed in 5-min bins by a trained observer blinded to the treatment condition. One scratch bout was defined as one or more rapid back-and-forth hind paw motions directed toward and contacting the injection site, ending with licking or biting of the toes or placement of the hind paw on the floor. Hind paw movements directed away from the injection site (e.g., ear-scratching) and grooming movements were not counted (Akiyama et al., 2009).

Hargreaves test

Mice were habituated to the Hargreaves arena for 120 min before testing. To determine the paw withdrawal latencies (PWLs), the plantar surface of the hind paws was exposed to five heat trials at 5-min intervals. PWL was measured both at baseline and during yellow light stimulation (2.0 mW, 2 Hz). The light was turned on during each trial of the Hargreaves' test. PWL was measured again 60 min after light stimulation. The beam active and idle intensities were 38 and 5, respectively. A cutoff of time of 10 s was used to prevent excessive tissue damage.

Hind paw withdrawal test

Mice were habituated to a perforated metal floor for 120 min before testing. The plantar surface of the hind paws was tested with a series of von Frey filaments (0.07–4 g) to determine the paw withdrawal threshold (PWT). PWT was determined before the light stimulation. After 30 min, mice were stimulated with yellow light (2.0 mW, 2 Hz) and their hind paws were tested. The light was turned on until the end of testing session. PWT was measured again 60 min after light stimulation. The strength (g) of the von Frey filament which induced paw withdrawal was noted for each stimulus.

Elevated plus maze

The elevated plus maze (EPM) was composed of four arms (4.5 cm wide × 30 cm long): two opposing "closed arms" surrounded on three sides with transparent, 18-cm-high walls; two opposing "open arms" with 1-cm-high ledges to prevent the mice from falling; and a central square. The entire apparatus was raised 32 cm from the floor. The experiments were conducted under normal lighting conditions (~100 lux).

Each mouse was weighed and acclimated to the testing room for at least 30 min before testing. Then, each mouse was placed into the center square of the EPM, facing an open arm, and video recorded for 9 min with recording divided into three 3-min epochs (OFF-ON-OFF or OFF-OFF-OFF) as previously shown (Felix-Ortiz et al., 2016; Sanders et al., 2019). The time interval between experiments with OFF-ON-OFF and OFF-OFF-OFF conditions was four weeks. Videos were analyzed by a trained observer blinded to the treatment group. A mouse was considered to have entered an arm when all four paws were placed on the floor in that arm. Decreased time in open arms was a considered measure of anxiety-like behavior, and the total number of entries was used as a general measure of locomotion (Rodgers and Johnson, 1995).

Open field test

The open field test (OFT) apparatus consisted of a large, square box (60 cm long × 60 cm wide × 40 cm high) with lines dividing the floor into 16 equal squares. The 12 squares adjacent to the wall were considered "peripheral," while the four squares in the middle of the floor were considered "central." The experiments were conducted under normal lighting.

As in the EPM, each mouse was weighed and acclimated to the testing room for at least 30 min before testing. Then, each mouse was placed into a corner of the OFT, facing parallel to a wall, and video recorded for 9 min with recording divided into three 3-min epochs (OFF-ON-OFF or

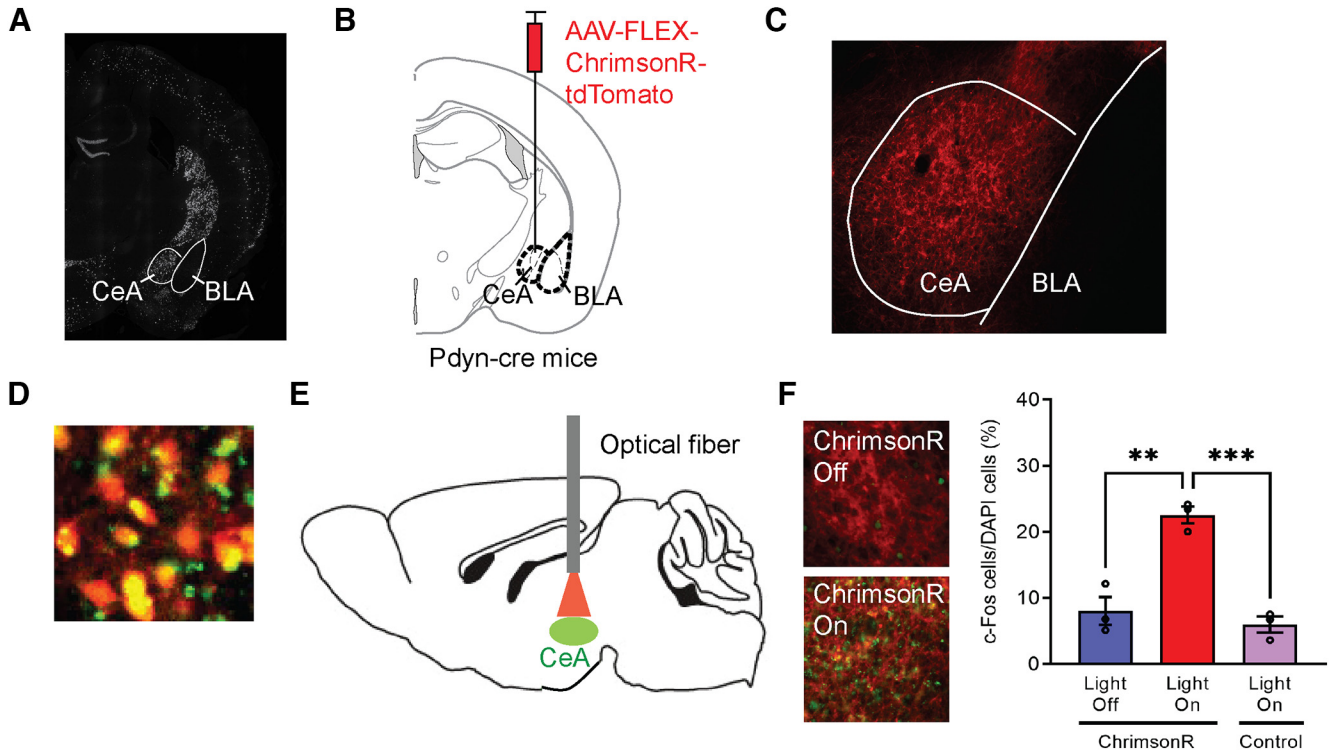

Figure 1. Optogenetic stimulation excited Pdyn$^+$ neurons in the central nucleus of the amygdala (CeA). ***A***, A representative image of coronal section of amygdala displays Pdyn mRNA signals detected by RNAscope in the CeA of C57BL/6 mice. ***B***, ***C***, Pdyn-cre mice received bilateral injections of AAV viruses containing the cre-dependent viral construct [AAV-FLEX-ChrimsonR-tdTomato or control (AAV-FLEX-tdTomato)] into the CeA. Schematic drawing shows a mouse brain coronal section [bregma: −1.34 (adapted from Franklin and Paxinos, 2008); ***B***]. Representative image shows tdTomato expression in the CeA (***C***). ***D***, A representative image of coronal section of amygdala showing immunoreactivity for Cre (green) and Pdyn$^+$ neurons (red). ***E***, Schematic of experimental procedure. Optic fibers were bilaterally implanted above the CeA. ***F***, Yellow light stimuli induced significant increases in the number of c-Fos$^+$ neurons (green) in the CeA of Pdyn-cre mice that received AAV-FLEX-ChrimsonR-tdTomato. Pdyn$^+$ neurons are shown in red. ($n = 3$/group), $F_{(2,6)} = 32$, $p = 0.0006$. Data are shown as mean ± SEM; $^{**}p < 0.01$, $^{***}p < 0.001$, for one-way ANOVA followed by Tukey's multiple comparison test.

OFF-OFF-OFF) as previously shown (Felix-Ortiz et al., 2016; Nishitani et al., 2019; Sanders et al., 2019). The time interval between experiments with OFF-ON-OFF and OFF-OFF-OFF conditions was four weeks. Videos were analyzed by a trained observer blinded to the treatment group. The number of entries into central and peripheral squares was counted. A mouse was considered to have entered a square when all four paws were placed on the floor in that square. Decreased percent entries into central squares (central/total) were considered a measure of anxiety-like behavior (Takahashi et al., 2006). The total number of square entries was used as a general measure of locomotion.

Immunohistochemistry

To confirm ChrimsonR function, c-Fos immunohistochemistry was used in combination with optic stimulation. Pdyn-Cre mice received bilateral injections of AAV into the CeA. An optic fiber was implanted directly above each injection site as described above. Two days before the experiment, mice had the toenails on their hind paws lightly trimmed to avoid the expression of c-Fos because of pain from scratching. On the experiment day, mice were weighed and habituated to the experiment room for 30 min. Then, each mouse was transferred to a quiet, familiar behavior chamber and received continuous bilateral yellow light stimulation for the entire period. Control mice did not receive light stimulation. After 2 h, mice were anesthetized with intraperitoneal sodium pentobarbital (80 mg/kg). Within 5–6 min of pentobarbital injection, mice were transcardially perfused with PBS, followed by 4% paraformaldehyde (PFA) in PBS.

To test the role of Pdyn$^+$ amygdaloid terminals in the PBN in itch signal processing, c-Fos immunohistochemistry was used in combination with optic stimulation. Pdyn-Cre mice received bilateral injections of AAV into the CeA. An optic fiber was implanted directly above PBN as described above. Two days before the experiment, mice had the toenails on their hind paws lightly trimmed. On the experiment day, mice were weighed and habituated to the experiment room for 30 min. Then, each mouse received an intradermal injection of PBS or chloroquine (100 μg/10 μl) into the rostral back skin with ("ON") and without ("OFF") continuous bilateral yellow light stimulation. Following injection, each mouse was transferred to a quiet, familiar behavior chamber for 2 h to allow for peak injection-induced c-Fos expression and to minimize neuronal activity from external stress (Akiyama et al., 2009; Gao and Ji, 2009; Sanders et al., 2019). After 2 h, mice were anesthetized with intraperitoneal sodium pentobarbital (80 mg/kg). Within 5–6 min of pentobarbital injection, mice were transcardially perfused with PBS, followed by 4% paraformaldehyde (PFA) in PBS.

Mouse brains were dissected and postfixed in 4% PFA overnight. For Cre staining, mouse brains were postfixed in 4% PFA for 4 h. Brains were cryoprotected in 30% sucrose for 24 h, frozen in Optimal Cutting Temperature compound (Sakura Finetek), and coronally sectioned at 40-μm thickness on a cryostat. Sections were stored in antifreeze solution at −20°C until staining.

For free-floating immunohistochemistry, sections were washed with PBS and then blocked with 5% normal donkey serum in PBS with 0.2% Triton X-100 for 2 h at room temperature. Sections were incubated with rabbit-anti-c-Fos primary antibody (1:1000; 5348T, RRID:AB_10557109; Cell Signaling Technology or 226003, RRID: AB_2231974; Synaptic Systems GmbH) in blocking buffer for 48 h at 4°C. For Cre staining, sections were incubated with rabbit-anti-Cre primary antibody (1:10,000; 69050-3, RRID:AB_2314229; Novagen) in blocking buffer for 48 h at 4°C. Following primary incubation, sections were washed with PBS, incubated with donkey-anti-rabbit secondary antibody conjugated with Alexa Fluor 488 (1:300, Invitrogen) in blocking buffer for 2 h at room temperature, washed again, and mounted on slides with Vectashield Hardset Antifade Mounting Medium with DAPI (Vector Laboratories).

Pilot studies were used to establish the sections with the highest c-Fos activity within the amygdala and PBN regions following itch stimulation. The following AP coordinates were chosen for quantification:

amygdala, −1.22, −1.34, and −1.46 mm from bregma; PBN, −5.02 and −5.20 mm. Of note, peak itch-evoked c-Fos PBN coordinates were consistent with previously reported results (Mu et al., 2017).

Stitched photomicrographs of whole sections were obtained using fluorescence microscopy (Leica Microsystems) at 10× objective magnification. For quantification, structural boundaries were drawn using ImageJ software with reference to Franklin and Paxinos (2008) and Vogt and Paxinos (2014). The number of c-Fos$^+$ neurons in each region of interest was counted manually by a trained observer blinded to the treatment condition.

RNAscope

C57BL/6J mice will be anesthetized with sodium pentobarbital (80 mg/kg), transcardially perfused with 4% PFA, and dissected. Brains were flash-frozen in 2-methylbutane and stored at −80°C. Brain sections containing the CeA were sectioned coronally at 16 µm with a cryostat. Sections were prepared for hybridization per the manufacturer's instructions (Advanced Cell Diagnostics, Inc) using probes for Pdyn (Mm-Pdyn-C3, catalog #318771). Stitched photomicrographs of whole sections were obtained using fluorescence microscopy (Leica Microsystems) at 10× objective magnification.

Statistical analysis

Results are presented as mean ± SEM. Statistical details of experiments can be found in figure legends. For comparison between two groups, a two-tailed Student's *t* test was used. For comparison among more than two groups, a one-way ANOVA followed by Tukey's multiple comparisons test was used. Statistical significance was set at $p < 0.05$ for all tests. All statistical analyses and graphs were made using GraphPad Prism9 (GraphPad Software).

Results

Optogenetic stimulation increases c-fos expression in Pdyn$^+$ amygdala neurons

Using RNAscope, we first investigated the distribution of Pdyn mRNA in the amygdala. As shown in Figure 1*A*, Pdyn+ cells were predominantly localized in CeA. To selectively express chrimsonR tagged with tdTomato in Pdyn+ CeA neurons, AAV-FLEX-chrimsonR-tdTomato was injected to the CeA of Pdyn-Cre mice (Fig. 1*B*). As shown in Figure 1*C*, chrimsonR-tdTomato-expressing cells were predominantly localized in CeA. To confirm that chrimsonR-tdTomato is only expressed in a Cre-dependent manner, double fluorescence imaging for Cre and tdTomato was performed. TdTomato expression was found in 76.9 ± 0.8% ($n = 3$) of Cre-expressing neurons, and tdTomato-expressing neurons always coexpressed Cre (Fig. 1*D*). To confirm the function of chrimsonR in the CeA, we looked at changes in the expression of the immediate early gene c-Fos after light stimulation of the CeA (Fig. 1*E*). In Pdyn-cre mice given AAV-FLEX-ChrimsonR-tdTomato, light stimulation significantly increased the number of c-Fos-positive cells (no light: 8.1 ± 2.1% of total neurons; light: 22.6 ± 1.3% of total neurons; $F_{(2,6)} = 32.43$, $p = 0.0006$; Tukey's *post hoc* test, $p = 0.0016$; Fig. 1*F*). Control mice did not exhibit this increase (Tukey's *post hoc* test, $p = 0.6504$; Fig. 1*F*). The c-Fos expression was found primarily in chrimsonR-tdTomato-expressing neurons (90.5 ± 1.6%, $n = 3$).

Optogenetic stimulation of Pdyn$^+$ amygdala neurons inhibits itch-related behavior and decreased the baseline heat sensitivity

To investigate whether optogenetic stimulation of Pdyn$^+$ amygdala neurons affects itch-related behavior, we videotaped mouse behaviors following intradermal injection of the pruritogens histamine and chloroquine with and without simultaneous light stimulation. Light stimulation of Pdyn$^+$ amygdala neurons significantly reduced the total scratching response to each pruritogen (Fig. 2*A*,*B*). Control mice exposed to the same light stimulation did not show a significant reduction in the total number of scratch bouts evoked by each pruritogen (Fig. 2*C*,*D*).

The Hargreaves test and von Frey filament test were used to determine whether optogenetic stimulation of Pdyn$^+$ amygdala neurons affects paw withdrawal behaviors. On the Hargreaves test, light stimulation of Pdyn$^+$ amygdala neurons increased withdrawal latencies (Fig. 2*E*). On the von Frey filament test, light stimulation had no significant effect on paw withdrawal thresholds (Fig. 2*F*). The same light stimulation had no significant effect on either paw withdrawal latencies or thresholds in control mice (Fig. 2*G*,*H*).

Collectively, these data demonstrate that optogenetic stimulation of Pdyn$^+$ amygdala neurons is capable of inhibiting itch-related behavior and decreasing the baseline heat sensitivity.

Optogenetic stimulation of Pdyn$^+$ amygdala neurons evokes anxiety-like behavior without reducing locomotion

Given that the CeA mediates itch-induced and pain-induced negative affect (Neugebauer, 2015; Sanders et al., 2019), we investigated whether optogenetic stimulation of Pdyn$^+$ amygdala neurons affects anxiety-like behavior. To measure anxiety-like behavior, we used the EPM and OFT that measure thigmotaxis: a preference toward contact with walls versus exploring unprotected spaces. On the EPM, mice showed a significant reduction in open arm time during light stimulation (Fig. 3*A*). Similarly, on the OFT, mice showed a significant reduction in percentage center entries during light stimulation (Fig. 3*C*). Optogenetic stimulation of Pdyn$^+$ amygdala neurons was not accompanied by a reduction in overall locomotion (Fig. 3*B*,*D*). Therefore, optogenetic stimulation of Pdyn$^+$ amygdala neurons was sufficient to enhance thigmotaxis. The same light stimulation had no significant effect on either open arm time or percentage center entries in control mice (Fig. 3*E*,*F*).

Optogenetic stimulation of Pdyn$^+$ amygdaloid terminals in the PBN inhibits itch-related behavior and decreased the baseline heat and mechanical sensitivity

Recent studies revealed that the CeA-PBN pathway is involved in pain regulation (Raver et al., 2020; Hogri et al., 2022). However, the contribution of Pdyn$^+$ CeA neurons to this inhibitory pathway has not been fully determined. To investigate this, we first examined the distribution of Pdyn$^+$ amygdaloid terminals in the PBN using Pdyn-Cre mice that received intra-amygdala injection of AAV-FLEX-chrimsonR-tdTomato (Fig. 4*A*). As shown in Figure 4*B*, chrimsonR-tdTomato expression was primarily found in the PBN. Next, we implanted optic fibers in the PBN to investigate whether optogenetic stimulation of Pdyn$^+$ amygdaloid terminals in the PBN affects itch-related behavior (Fig. 4*A*). Mouse behaviors were videotaped following intradermal injection of the pruritogens histamine and chloroquine with and without simultaneous light stimulation. The total scratching response to each pruritogen was significantly reduced by light stimulation of Pdyn$^+$ amygdaloid terminals in the PBN (Fig. 4*C*,*D*). Control mice exposed to the same light stimulation did not show a significant reduction in the total number of scratch bouts evoked by each pruritogen (Fig. 4*E*,*F*).

The Hargreaves test and von Frey filament test were used to determine whether optogenetic stimulation of Pdyn$^+$ amygdaloid terminals in the PBN affects paw withdrawal behaviors. On

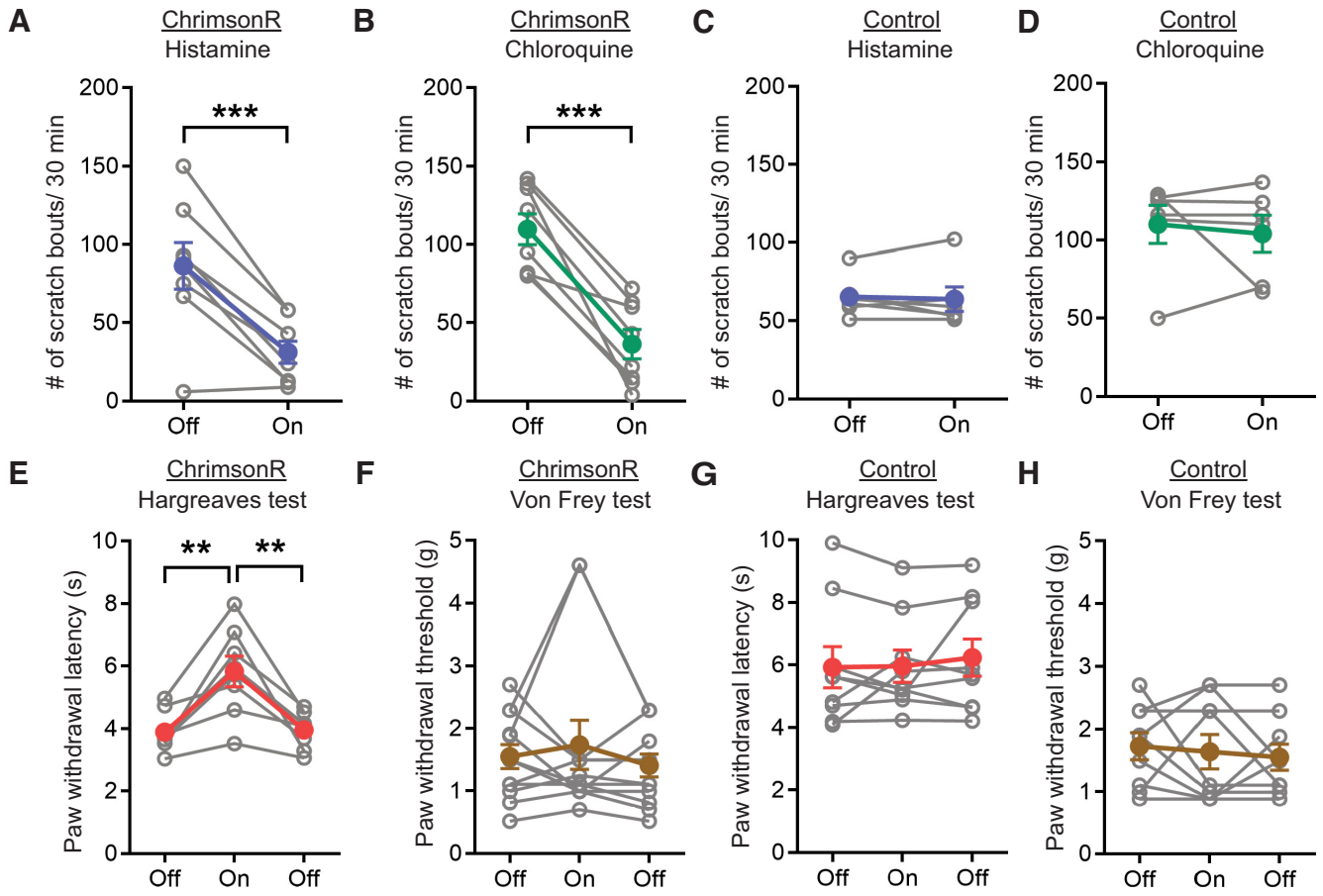

Figure 2. Optogenetic stimulation of Pdyn$^+$ amygdala neurons inhibited itch-related behavior and thermal pain-related behavior. ***A***, Number of scratch bouts/30 min after intradermal injection of histamine in Pdyn-cre mice that received AAV-FLEX-ChrimsonR-tdTomato with or without light stimuli. Mice received bilateral intra-CeA injections of AAV-FLEX-ChrimsonR-tdTomato. Optic fibers were implanted above the CeA. $n = 8$/group, $t_{(7)} = 5.530$, $p = 0.0009$. ***B***, As in ***A***, for intradermal chloroquine in Pdyn-cre mice that received AAV-FLEX-ChrimsonR-tdTomato ($n = 8$/group), $t_{(7)} = 6.900$, $p = 0.0002$. ***C***, As in ***A***, for intradermal histamine in Pdyn-cre mice that received AAV-FLEX-tdTomato (control). $n = 6$/group, $t_{(5)} = 0.3983$, $p = 0.7069$. ***D***, As in ***A***, for intradermal chloroquine in control mice. $n = 6$/group, $t_{(5)} = 0.5109$, $p = 0.6312$. ***E***, Paw withdrawal latency in Pdyn-cre mice that received AAV-FLEX-ChrimsonR-tdTomato. The Hargreaves test was performed before, during, and after bilateral light stimulation ($n = 8$/group), $F_{(1.476,10.33)} = 17.6$, $p = 0.0008$. ***F***, Paw withdrawal threshold in Pdyn-cre mice that received AAV-FLEX-ChrimsonR-tdTomato. The von Frey filament test was performed before, during, and after bilateral light stimulation ($n = 12$/group), $F_{(1.213,13.35)} = 0.7305$, $p = 0.4339$. ***G***, As in ***E*** for control mice. $n = 8$/group. $F_{(1.885,15.08)} = 0.2246$, $p = 0.7890$. ***H***, As in ***F*** for control mice. $n = 8$/group. $F_{(1.865,14.92)} = 0.4417$, $p = 0.6376$. Data are shown as mean ± SEM; ***$p < 0.001$, for paired t test versus light off (***A***, ***B***). **$p < 0.01$, for one-way repeated measures ANOVA followed by Tukey's multiple comparison test versus light off (***E***, ***F***).

the Hargreaves test, light stimulation of Pdyn$^+$ amygdaloid terminals in the PBN increased withdrawal latencies (Fig. 4*G*). Likewise, on the von Frey filament test, light stimulation increased paw withdrawal thresholds (Fig. 4*H*). The same light stimulation had no significant effect on either paw withdrawal latencies or thresholds in control mice (Fig. 4*I*,*J*).

Taken together, these data demonstrate that optogenetic stimulation of Pdyn$^+$ amygdaloid terminals in the PBN is capable of inhibiting itch-related behavior while also decreasing the baseline heat and mechanical sensitivities.

Optogenetic stimulation of Pdyn$^+$ amygdaloid terminals in the PBN evokes anxiety-like behavior without reducing locomotion

To investigate whether optogenetic stimulation of Pdyn$^+$ amygdaloid terminals in the PBN affects anxiety-like behavior, we used the EPM and OFT. Light stimulation had no effect on open arm time as measured by the EPM (Fig. 5*A*). Similarly, on the OFT, light stimulation had no effect on percentage center entries (Fig. 5*C*). Optogenetic stimulation of Pdyn$^+$ amygdaloid terminals in the PBN significantly reduced total arm entries during light stimulation (Fig. 5*B*). However, light stimulation had no effect on total square entries (Fig. 5*D*). The same light stimulation had no significant effect on either open arm time or percentage center entries in control (Fig. 5*E*,*F*). Overall, optogenetic stimulation of Pdyn$^+$ amygdaloid terminals in the PBN was insufficient to enhance thigmotaxis.

Optogenetic stimulation of Pdyn$^+$ amygdaloid terminals in the PBN decreases chloroquine-induced c-fos expression in the PBN

Recent studies have revealed that the PBN functions as an important relay center in the process of itch information (Jansen and Giesler, 2015; Akiyama et al., 2016; Mu et al., 2017). To test whether optogenetic stimulation of Pdyn$^+$ amygdaloid terminals in the PBN regulates itch-responsive neurons in the PBN, we evaluated c-fos expression in the PBN. Chloroquine significantly increased the number of c-fos-positive cells (PBS OFF: 3.5 ± 1.2 in PBNLE, 27.4 ± 7.9 in PBN; Chloroquine OFF: 22.0 ± 2.0 in PBNLE, 127.5 ± 18.3 in PBN; Fig. 6*A*,*B*). Chloroquine-induced c-fos expression was significantly reduced by light stimulation in Pdyn-cre mice that received AAV-FLEX-ChrimsonR-tdTomato (Chloroquine ON: 5.0 ± 0.9 in PBNLE, 31.3 ± 1.9 in PBN; Fig. 6*A*,*B*). This reduction was not observed in

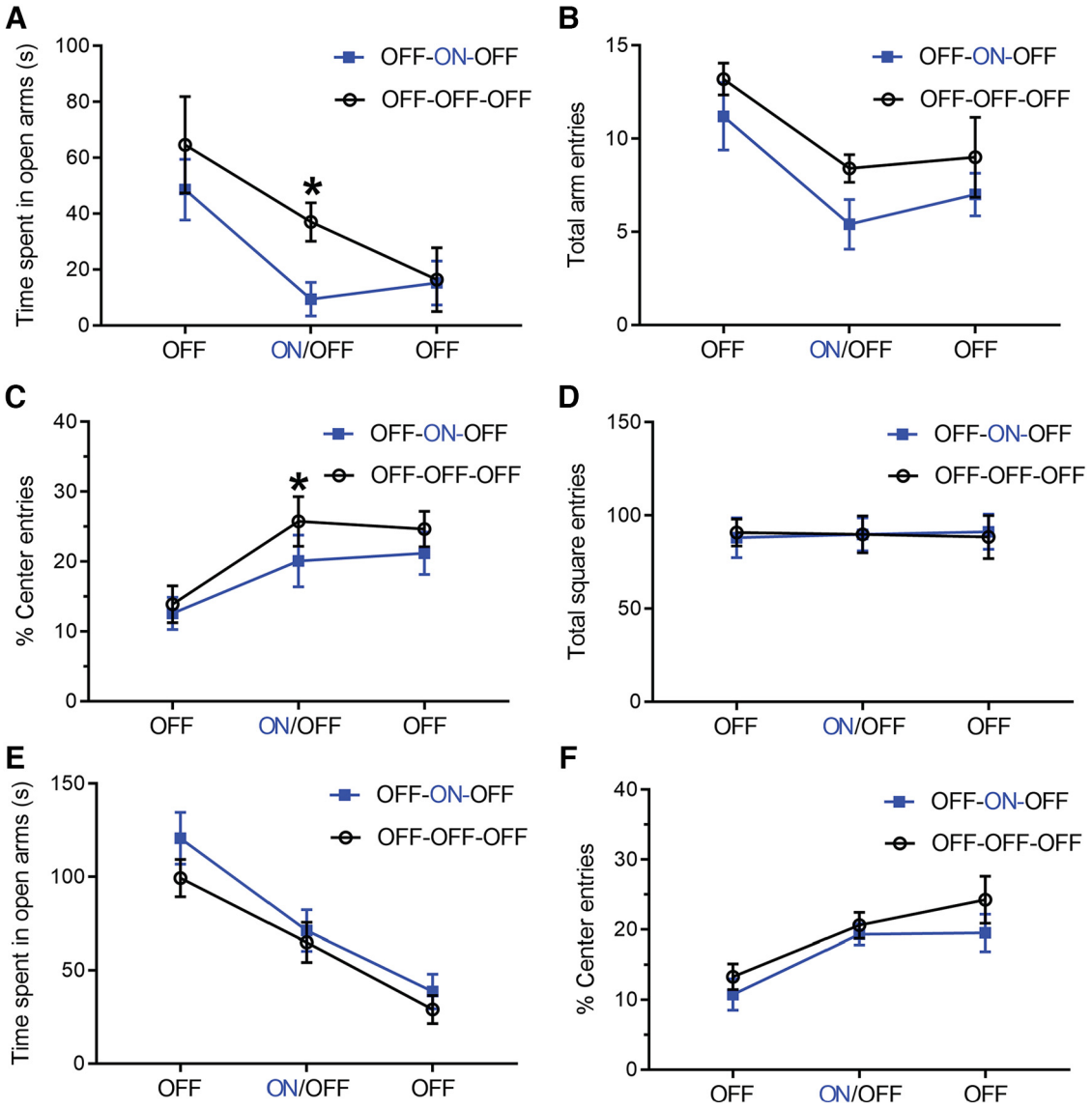

Figure 3. Optogenetic stimulation of Pdyn$^+$ amygdala neurons evoked anxiety-like behavior. Pdyn-cre mice received bilateral intra-CeA injections of either AAV-FLEX-ChrimsonR-tdTomato or AAV-FLEX-tdTomato (control). Optic fibers were implanted above the CeA. The EPM and OFT tests were performed under light off and on conditions. ***A***, On the EPM, yellow light stimulation reduced open arm time, a measure of thigmotaxis, in Pdyn-cre mice that received AAV-FLEX-ChrimsonR-tdTomato ($n = 5$/group), $t_{(4)} = 3.165$, $p = 0.034$. ***B***, On the EPM, yellow light stimulation did not affect the total number of arm entries, a measure of locomotion in Pdyn-cre mice that received AAV-FLEX-ChrimsonR-tdTomato ($n = 5$/group), $t_{(4)} = 2.449$, $p = 0.070$. ***C***, On the OFT, yellow light stimulation induced a reduction in the percentage of center square entries, another measure of thigmotaxis, in Pdyn-cre mice that received AAV-FLEX-ChrimsonR-tdTomato ($n = 5$/group), $t_{(4)} = 2.811$, $p = 0.048$. ***D***, On the OFT, yellow light stimulation did not affect the total number of square entries, another measure of locomotion, in Pdyn-cre mice that received AAV-FLEX-ChrimsonR-tdTomato ($n = 5$/group), $t_{(4)} = 0.000$, $p > 0.9999$. ***E***, As in ***A*** for control mice ($n = 9$/group), $t_{(8)} = 0.3152$, $p = 0.775$. ***F***, As in ***C*** for control mice ($n = 9$/group), $t_{(8)} = 0.678$, $p = 0.522$. All experiments were performed under light off and on conditions. Data are shown as mean ± SEM; *$p < 0.05$, for paired *t* test versus light off.

control mice [Chloroquine ON (control): 26.8 ± 1.8 in PBNLE, 136.8 ± 10.7 in PBN; Fig. 6*B*]. Collectively, these results suggest that optogenetic stimulation of Pdyn$^+$ amygdaloid terminals in the PBN regulates itch by inhibiting itch-signaling neurons in the PBN.

Discussion

PBN receives direct inputs from spinal neurons and serves as an important relay hub for itch and pain signal processing (Han et al., 2015; Neugebauer, 2015; Akiyama et al., 2016; Mu et al., 2017; Campos et al., 2018). A recent study demonstrated that the CeA-PBN pathway is involved in the regulation of pain signaling (Raver et al., 2020). Our results extend this previous finding by showing that optogenetic stimulation of Pdyn$^+$ amygdaloid terminals in the PBN is sufficient to inhibit paw withdrawal behaviors. Moreover, we show that Pdyn$^+$ CeA to PBN-projecting neurons regulate itch-related behaviors by inhibiting itch signaling in the PBN (Fig. 7).

Optogenetic stimulation of Crh$^+$ CeA-PBN projections has been reported to increase mechanical threshold in basal conditions (Raver et al., 2020). Another study showed that optogenetic stimulation of CaMKIIa$^+$ CeA-PBN projections increased thermal and mechanical thresholds in basal conditions (Hogri et al., 2022). Consistent with previous findings, we found that optogenetic stimulation of Pdyn$^+$ CeA-PBN projections increased thermal and mechanical thresholds in basal conditions. Previous studies investigated the roles of CeA-PBN projections in thermal hyperalgesia and mechanical allodynia (Raver et al., 2020;

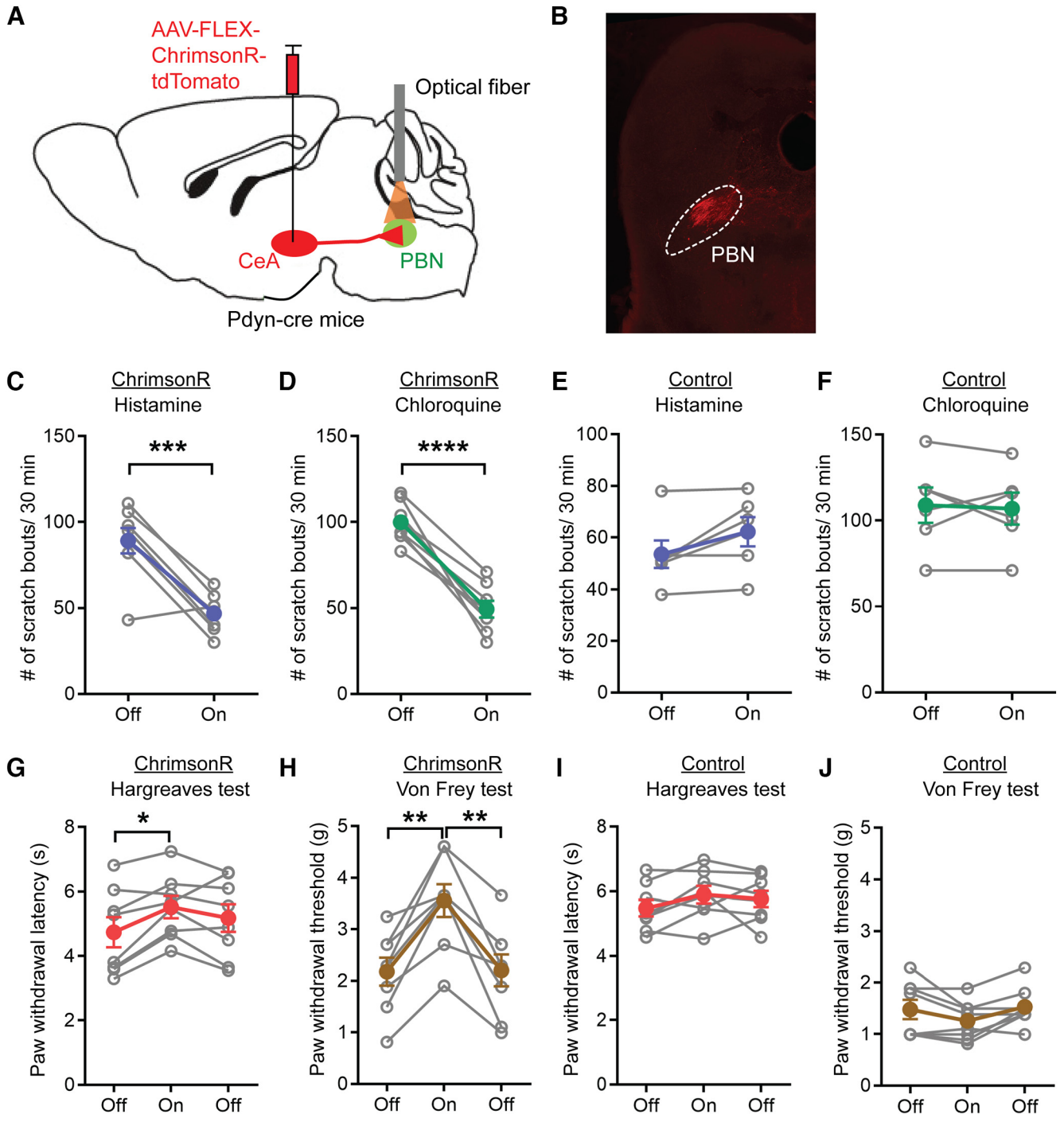

Figure 4. Optogenetic stimulation of Pdyn^{+} amygdaloid terminals in the PBN inhibited itch-related and pain-related behaviors. ***A***, Schematic of experimental procedure. Pdyn-cre mice received bilateral intra-CeA injections of either AAV-FLEX-ChrimsonR-tdTomato or AAV-FLEX-tdTomato (control). Optic fibers were implanted above the PBN. ***B***, Representative image of coronal section of PBN of Pdyn-cre mice that received injection of AAV-FLEX-ChrimsonR-tdTomato into CeA. Abundant axons expressing tdTomato are observed in the PBN. ***C***, Number of scratch bouts after intradermal injection of histamine in Pdyn-cre mice that received AAV-FLEX-ChrimsonR-tdTomato with or without light stimuli ($n = 8$/group), $t_{(7)} = 5.681$, $p = 0.0008$. ***D***, As in ***C***, for intradermal chloroquine ($n = 8$/group). ***E***, As in ***C***, for intradermal histamine in Pdyn-cre mice that received AAV-FLEX-tdTomato (control). $n = 6$/group, $t_{(5)} = 2.039$, $p = 0.097$. ***F***, As in ***D***, for intradermal chloroquine in control mice. $n = 6$/group, $t_{(5)} = 0.3057$, $p = 0.7721$. ***G***, Paw withdrawal latency in Pdyn-cre mice that received AAV-FLEX-ChrimsonR-tdTomato. The Hargreaves test was performed before, during, and after bilateral light stimulation ($n = 8$/group), $F_{(1.917,13.42)} = 6.432$, $p = 0.0116$. ***H***, Paw withdrawal threshold in Pdyn-cre mice that received AAV-FLEX-ChrimsonR-tdTomato. The von Frey filament test was performed before, during, and after bilateral light stimulation ($n = 8$/group), $F_{(1.942,13.60)} = 17.72$, $p = 0.0002$. ***I***, As in ***G*** for control mice. $n = 8$/group. $F_{(1.333,9.332)} = 2.631$, $p = 0.1339$. ***J***, As in ***H*** for control mice. $n = 8$/group. $F_{(1.736,12.15)} = 2.224$, $p = 0.1538$. Data are shown as mean ± SEM; ***$p < 0.001$, ****$p < 0.0001$, for paired *t* test versus light off (***C***, ***D***). *$p < 0.05$, **$p < 0.01$, for one-way repeated measures ANOVA followed by Tukey's multiple comparison test versus light off (***G***, ***H***).

Hogri et al., 2022). Optogenetic stimulation of Crh^{+} CeA-PBN projections inhibited formalin-induced mechanical allodynia, whereas optogenetic stimulation of CaMKIIa^{+} CeA-PBN projections inhibited capsaicin-induced thermal hyperalgesia and mechanical allodynia. CeA-PBN projections appear to be involved in pain signal regulation under inflammatory pain conditions.

In this study, we investigated the effects of optogenetic stimulation on Pdyn+ neurons in the CeA and their influence on paw

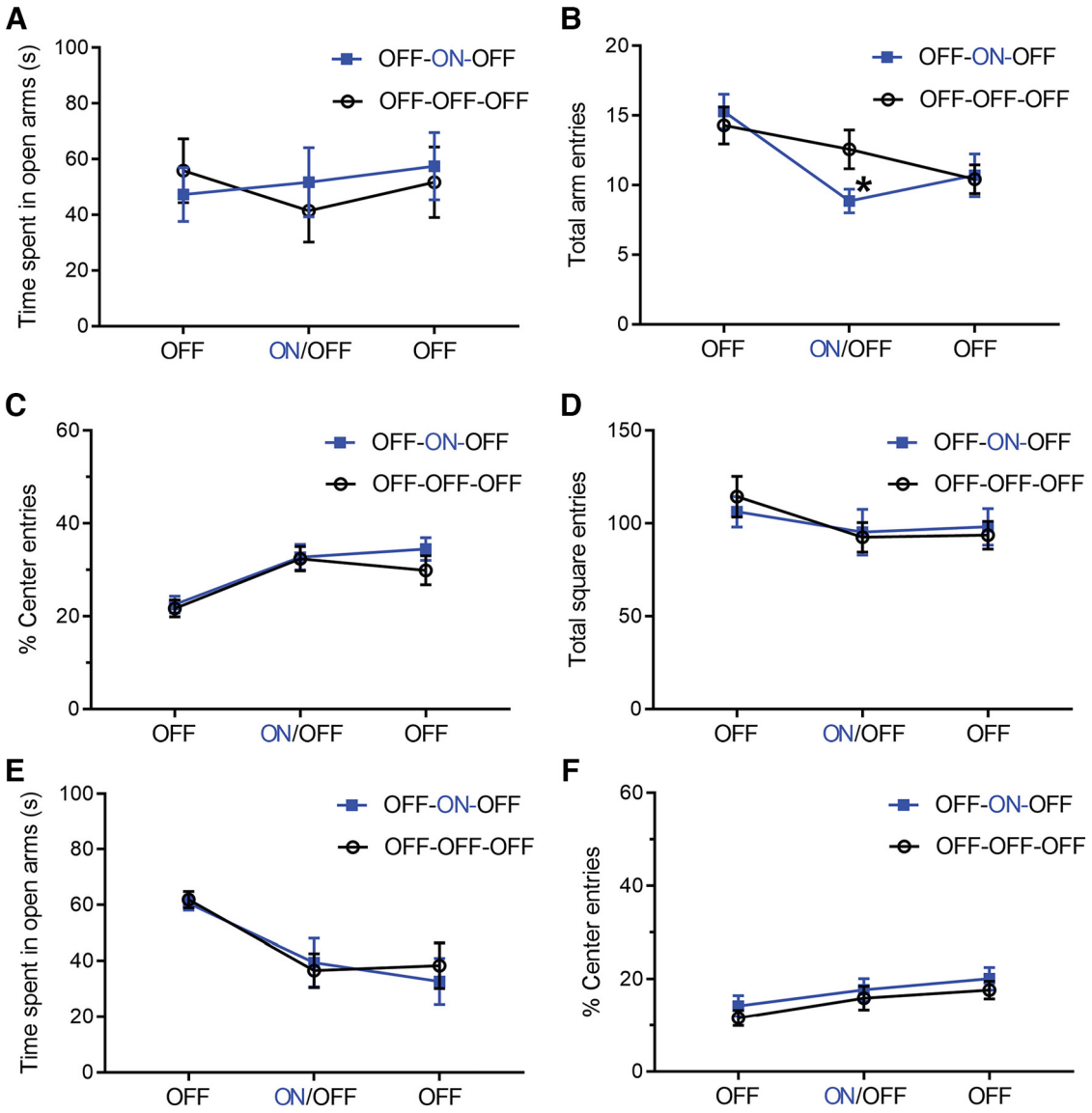

Figure 5. Optogenetic stimulation of Pdyn$^+$ amygdaloid terminals in the PBN did not affect anxiety-like behavior. Pdyn-cre mice received bilateral intra-CeA injections of either AAV-FLEX-ChrimsonR-tdTomato or AAV-FLEX-tdTomato (control). Optic fibers were implanted above the PBN. The EPM and OFT tests were performed under light off and on conditions. ***A***, On the EPM, yellow light stimulation did not affect open arm time, a measure of thigmotaxis, in Pdyn-cre mice that received AAV-FLEX-ChrimsonR-tdTomato ($n = 8$/group), $t_{(7)} = 0.230$, $p = 0.8250$. ***B***, On the EPM, yellow light stimulation reduced the total number of arm entries, a measure of locomotion, in Pdyn-cre mice that received AAV-FLEX-ChrimsonR-tdTomato ($n = 8$/group), $t_{(7)} = 3.048$, $p = 0.0186$. ***C***, On the OFT, yellow light stimulation did not affect the percentage of center square entries, another measure of thigmotaxis, in Pdyn-cre mice that received AAV-FLEX-ChrimsonR-tdTomato ($n = 8$/group), $t_{(7)} = 0.0965$, $p = 0.9258$. ***D***, On the OFT, yellow light stimulation did not affect the total number of square entries, another measure of locomotion, in Pdyn-cre mice that received AAV-FLEX-ChrimsonR-tdTomato ($n = 8$/group), $t_{(7)} = 0.3356$, $p = 0.7470$. ***E***, As in ***A*** for control mice ($n = 8$/group), $t_{(7)} = 0.3346$, $p = 0.954$. ***F***, As in ***C*** for control mice ($n = 8$/group), $t_{(7)} = 1.455$, $p = 0.191$. Data are shown as mean ± SEM; *$p < 0.05$, for paired *t* test versus light off.

withdrawal thresholds in response to mechanical stimuli. Intriguingly, we observed that the activation of these neurons did not yield any significant alterations in mechanical thresholds. However, when we specifically activated the terminals of these neurons that project to the PBN, we noted an increase in mechanical thresholds. This contrasting outcome implies the involvement of a subset of CeA neurons that play a role in reducing mechanical thresholds and do not have projections to the PBN. One potential candidate for these neurons is the PKCδ^+ CeA neurons, which, when chemogenetically activated, promote tactile sensitivity while leaving thermal thresholds unaffected in basal conditions (Wilson et al., 2019). Furthermore, PKCδ^+ CeA neurons have been observed to exhibit few projections to the PBN (O'Leary et al., 2022). To explore their potential involvement, we investigated the overlap between Pdyn$^+$ and PKCδ^+ CeA neurons in 22 CeA cell clusters, categorized by molecular marker genes and projection types, using fluorescence in situ hybridization data (Wang et al., 2023). Among these clusters, we found that 22% (218/977) of molecular cluster 2, uniquely marked by Vipr2, expressed both Pdyn and Prkcd (encoding PKCδ). However, further studies are necessary to determine whether this specific subpopulation of CeA neurons is sufficient to promote tactile sensitivity.

Glutaminergic excitatory neurons project from the PBN to the CeA (Neugebauer, 2015). PBN-to-CeA-projecting neurons target somatostatin-expressing CeA neurons, which play a role in pain signal regulation (Wilson et al., 2019; Li and Sheets, 2020). Additionally, somatostatin-expressing CeA neurons project to PBN and overlap with dynorphin-expressing neurons in

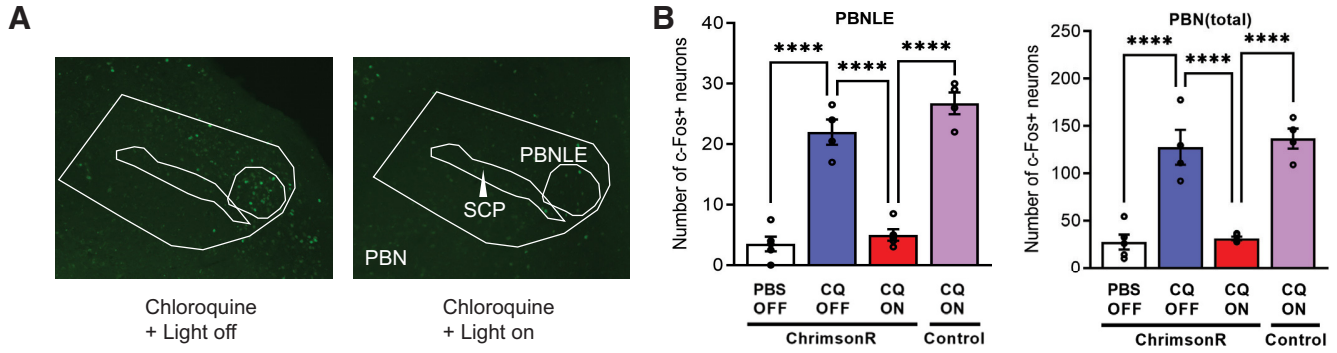

Figure 6. Optogenetic stimulation of Pdyn$^+$ amygdaloid terminals in the PBN reduced neuronal activity associated with acute itch. ***A***, Representative images of c-Fos immunostaining in PBN following intradermal injection of chloroquine with or without light stimulation. PBNLE and superior cerebellar peduncle (SCP) are indicated for PBN. ***B***, Quantification of c-Fos+ neurons in PBN following intradermal PBS and CQ (chloroquine) with or without light stimulation in Pdyn-cre mice that received AAV-FLEX-ChrimsonR-tdTomato or AAV-FLEX-tdTomato (control). PBNLE: $F_{(3,14)} = 62.93$, $p < 0.0001$. Total PBN: $F_{(3,14)} = 32.76$, $p < 0.0001$. Data in ***B*** are shown as mean ± SEM; ****$p < 0.0001$ for Tukey's multiple comparisons test.

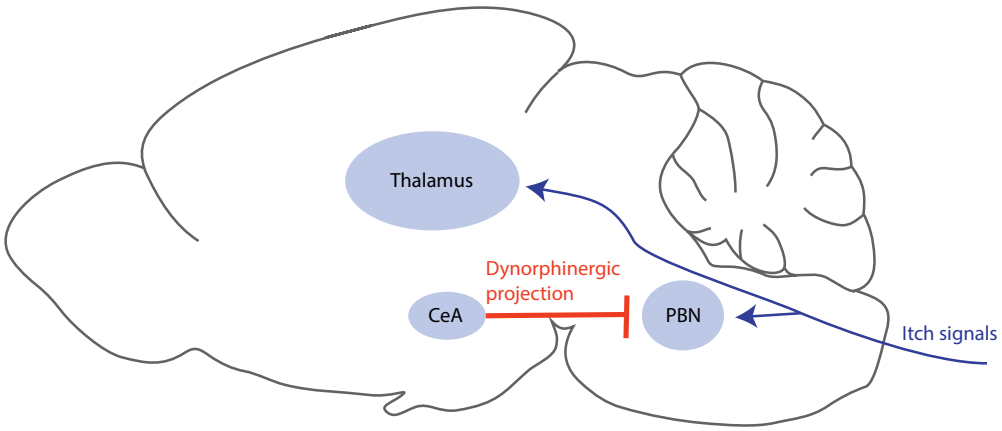

Figure 7. A subset of the central amygdala (CeA) neurons regulates itch signaling. Pdyn$^+$ CeA neurons send projections to the parabrachial nucleus (PBN). Optogenetic stimulation of Pdyn$^+$ CeA-PBN projections reduces itch-related behaviors.

the CeA (Kim et al., 2017; Raver et al., 2020). Therefore, Pdyn$^+$ CeA neurons are most likely involved in regulating itch and pain signaling via feedback inhibition of the PBN-to-CeA-projecting neurons.

We previously discovered that a subpopulation of amygdala neurons that respond to itch plays a role in increasing itch-related behaviors (Sanders et al., 2019). Given that intraamygdala injection of the $GABA_A$ agonist was reported to reduce itch-related behaviors (Chen et al., 2016), these itch responsive amygdala neurons appeared to be under the control of GABAergic neurons. In this study, we found that Pdyn$^+$ CeA-PBN-projecting neurons are involved in the regulation of itch-related behaviors. Given that most of all CeA neurons are GABAergic inhibitory neurons (Janak and Tye, 2015; Li and Sheets, 2020), itch-responsive amygdala neurons enhance itch by inhibiting the itch inhibitory pathway, which could be the Pdyn$^+$ CeA-PBN pathway. Another possibility is that itch-responsive amygdala neurons inhibit GABAergic neurons in the PAG. It was reported that reactivating the itch-responsive CeA-PAG projection was sufficient to induce itch-related behaviors (Samineni et al., 2021). Chemogenetic inhibition of GABAergic neurons in the PAG has been shown to increase itch-related behaviors (Samineni et al., 2019). Further research is needed to elucidate how the amygdala processes itch signaling.

In this study, we showed that optogenetic stimulation of Pdyn$^+$ amygdala neurons elicited anxiety-like behaviors. Similarly, optogenetic stimulation of Pdyn$^+$ amygdala neurons promoted aversive behaviors (McCall et al., 2018). In view of the fact that the optogenetic stimulation of Pdyn$^+$ amygdaloid terminals in the PBN had no effect on anxiety-like behaviors, Pdyn$^+$ amygdala projection to another brain area is presumably involved in negative affect. This idea is supported by a previous study showing that the CeA-bed nucleus of the stria terminalis pathway contains dynorphin and facilitates anxiety-like behaviors (Ahrens et al., 2018).

A previous study showed that optogenetic stimulation of CaMKIIα^+ CeA-PBN-projecting neurons can reduce thigmotaxis behaviors (Hogri et al., 2022). Optogenetic stimulation of Pdyn$^+$ CeA-PBN-projecting neurons, on the other hand, did not reduce thigmotaxis behaviors. This difference is probably caused by the neurochemical and functional heterogeneity of the CeA-PBN pathway (Raver et al., 2020). CaMKIIα^+ CeA-PBN-projecting neurons are a subset of somatostatin-expressing neurons that account for 26% of CeA-PBN-projecting neurons (Hogri et al., 2022). Pdyn$^+$ CeA-PBN-projecting neurons account for 42% of all projection neurons. Somatostatin is expressed by ~40% of them (Raver et al., 2020). It is plausible that two different populations of CeA-PBN-projecting neurons play different roles in thigmotaxis behaviors.

This study has shown that optogenetic stimulation of Pdyn$^+$ CeA can reduce itch signaling in the PBN by activating Pdyn$^+$ amygdaloid terminals in the PBN. The findings reported here

shed new light on the role of the CeA-PBN pathway in itch signal processing.

References

Ahrens S, Wu MV, Furlan A, Hwang GR, Paik R, Li H, Penzo MA, Tollkuhn J, Li B (2018) A central extended amygdala circuit that modulates anxiety. J Neurosci 38:5567–5583.

Akiyama T, Merrill AW, Zanotto K, Carstens MI, Carstens E (2009) Scratching behavior and Fos expression in superficial dorsal horn elicited by protease-activated receptor agonists and other itch mediators in mice. J Pharmacol Exp Ther 329:945–951.

Akiyama T, Curtis E, Nguyen T, Carstens MI, Carstens E (2016) Anatomical evidence of pruriceptive trigeminothalamic and trigeminoparabrachial projection neurons in mice. J Comp Neurol 524:244–256.

Bartonjo JJ, Lundy RF (2020) Distinct populations of amygdala somatostatin-expressing neurons project to the nucleus of the solitary tract and parabrachial nucleus. Chem Senses 45:687–698.

Cai YQ, Wang W, Paulucci-Holthauzen A, Pan ZZ (2018) Brain circuits mediating opposing effects on emotion and pain. J Neurosci 38:6340–6349.

Campos CA, Bowen AJ, Roman CW, Palmiter RD (2018) Encoding of danger by parabrachial CGRP neurons. Nature 555:617–622.

Chen L, Wang W, Tan T, Han H, Dong Z (2016) GABA(A) receptors in the central nucleus of the amygdala are involved in pain- and itch-related responses. J Pain 17:181–189.

Chiang MC, Nguyen EK, Canto-Bustos M, Papale AE, Oswald AM, Ross SE (2020) Divergent neural pathways emanating from the lateral parabrachial nucleus mediate distinct components of the pain response. Neuron 106:927–939.e5.

Deng J, Zhou H, Lin JK, Shen ZX, Chen WZ, Wang LH, Li Q, Mu D, Wei YC, Xu XH, Sun YG (2020) The parabrachial nucleus directly channels spinal nociceptive signals to the intralaminar thalamic nuclei, but not the amygdala. Neuron 107:909–923.e6.

Felix-Ortiz AC, Burgos-Robles A, Bhagat ND, Leppla CA, Tye KM (2016) Bidirectional modulation of anxiety-related and social behaviors by amygdala projections to the medial prefrontal cortex. Neuroscience 321:197–209.

Franklin KB, Paxinos G (2008) The mouse brain in stereotaxic coordinates, Ed 3 San Diego: Academic.

Gao YJ, Ji RR (2009) c-Fos and pERK, which is a better marker for neuronal activation and central sensitization after noxious stimulation and tissue injury? Open Pain J 2:11–17.

Han S, Soleiman MT, Soden ME, Zweifel LS, Palmiter RD (2015) Elucidating an affective pain circuit that creates a threat memory. Cell 162:363–374.

Hardaway JA, et al. (2019) Central amygdala prepronociceptin-expressing neurons mediate palatable food consumption and reward. Neuron 102:1037–1052.e7.

Hogri R, Teuchmann HL, Heinke B, Holzinger R, Trofimova L, Sandkühler J (2022) GABAergic CaMKIIα+ amygdala output attenuates pain and modulates emotional-motivational behavior via parabrachial inhibition. J Neurosci 42:5373–5388.

Hua T, Chen B, Lu D, Sakurai K, Zhao S, Han BX, Kim J, Yin L, Chen Y, Lu J, Wang F (2020) General anesthetics activate a potent central pain-suppression circuit in the amygdala. Nat Neurosci 23:854–868.

Janak PH, Tye KM (2015) From circuits to behaviour in the amygdala. Nature 517:284–292.

Jansen NA, Giesler GJ Jr (2015) Response characteristics of pruriceptive and nociceptive trigeminoparabrachial tract neurons in the rat. J Neurophysiol 113:58–70.

Kim J, Zhang X, Muralidhar S, LeBlanc SA, Tonegawa S (2017) Basolateral to central amygdala neural circuits for appetitive behaviors. Neuron 93:1464–1479.e5.

Klapoetke NC, et al. (2014) Independent optical excitation of distinct neural populations. Nat Methods 11:338–346.

Li JN, Sheets PL (2020) Spared nerve injury differentially alters parabrachial monosynaptic excitatory inputs to molecularly specific neurons in distinct subregions of the central amygdala. Pain 161:166–176.

McCall J, Walicki M, Norris M, Copits B, Meaden R, Gereau R (2018) Determining the response of central amygdala dynorphin neurons to stress and pain. J Pain 19:S9–S10.

Mochizuki H, Hernandez L, Yosipovitch G, Sadato N, Kakigi R (2020) The amygdala network for processing itch in human brains. Acta Derm Venereol 100:adv00345.

Mu D, Deng J, Liu KF, Wu ZY, Shi YF, Guo WM, Mao QQ, Liu XJ, Li H, Sun YG (2017) A central neural circuit for itch sensation. Science 357:695–699.

Neugebauer V (2015) Amygdala pain mechanisms. Handb Exp Pharmacol 227:261–284.

Nishitani N, Nagayasu K, Asaoka N, Yamashiro M, Andoh C, Nagai Y, Kinoshita H, Kawai H, Shibui N, Liu B, Hewinson J, Shirakawa H, Nakagawa T, Hashimoto H, Kasparov S, Kaneko S (2019) Manipulation of dorsal raphe serotonergic neurons modulates active coping to inescapable stress and anxiety-related behaviors in mice and rats. Neuropsychopharmacology 44:721–732.

Oh SW, et al. (2014) A mesoscale connectome of the mouse brain. Nature 508:207–214.

O'Leary TP, Kendrick RM, Bristow BN, Sullivan KE, Wang L, Clements J, Lemire AL, Cembrowski MS (2022) Neuronal cell types, projections, and spatial organization of the central amygdala. iScience 25:105497.

Papoiu AD, Coghill RC, Kraft RA, Wang H, Yosipovitch G (2012) A tale of two itches. Common features and notable differences in brain activation evoked by cowhage and histamine induced itch. Neuroimage 59:3611–3623.

Raver C, Uddin O, Ji Y, Li Y, Cramer N, Jenne C, Morales M, Masri R, Keller A (2020) An amygdalo-parabrachial pathway regulates pain perception and chronic pain. J Neurosci 40:3424–3442.

Rodgers RJ, Johnson NJ (1995) Factor analysis of spatiotemporal and ethological measures in the murine elevated plus-maze test of anxiety. Pharmacol Biochem Behav 52:297–303.

Samineni VK, Grajales-Reyes JG, Sundaram SS, Yoo JJ, Gereau RW 4th (2019) Cell type-specific modulation of sensory and affective components of itch in the periaqueductal gray. Nat Commun 10:4356.

Samineni VK, Grajales-Reyes JG, Grajales-Reyes GE, Tycksen E, Copits BA, Pedersen C, Ankudey ES, Sackey JN, Sewell SB, Bruchas MR, Gereau RW (2021) Cellular, circuit and transcriptional framework for modulation of itch in the central amygdala. Elife 10:e68130.

Sanders KM, Akiyama T (2018) The vicious cycle of itch and anxiety. Neurosci Biobehav Rev 87:17–26.

Sanders KM, Sakai K, Henry TD, Hashimoto T, Akiyama T (2019) A subpopulation of amygdala neurons mediates the affective component of itch. J Neurosci 39:3345–3356.

Simons LE, Moulton EA, Linnman C, Carpino E, Becerra L, Borsook D (2014) The human amygdala and pain: evidence from neuroimaging. Hum Brain Mapp 35:527–538.

Takahashi A, Kato K, Makino J, Shiroishi T, Koide T (2006) Multivariate analysis of temporal descriptions of open-field behavior in wild-derived mouse strains. Behav Genet 36:763–774.

Torruella-Suárez ML, Vandenberg JR, Cogan ES, Tipton GJ, Teklezghi A, Dange K, Patel GK, McHenry JA, Hardaway JA, Kantak PA, Crowley NA, DiBerto JF, Faccidomo SP, Hodge CW, Stuber GD, McElligott ZA (2020) Manipulations of central amygdala neurotensin neurons alter the consumption of ethanol and sweet fluids in mice. J Neurosci 40:632–647.

Vierow V, Forster C, Vogelgsang R, Dörfler A, Handwerker HO (2015) Cerebral networks linked to itch-related sensations induced by histamine and capsaicin. Acta Derm Venereol 95:645–652.

Vogt BA, Paxinos G (2014) Cytoarchitecture of mouse and rat cingulate cortex with human homologies. Brain Struct Funct 219:185–192.

Wang Y, Krabbe S, Eddison M, Henry FE, Fleishman G, Lemire AL, Wang L, Korff W, Tillberg PW, Lüthi A, Sternson SM (2023) Multimodal mapping of cell types and projections in the central nucleus of the amygdala. Elife 12:e84262.

Wilson TD, Valdivia S, Khan A, Ahn HS, Adke AP, Martinez Gonzalez S, Sugimura YK, Carrasquillo Y (2019) Dual and opposing functions of the central amygdala in the modulation of pain. Cell Rep 29:332–346.e5.